

# Towards a 1.5 MW, 140 GHz gyrotron for the upgraded ECRH system at W7-X

Konstantinos A. Avramidis<sup>a</sup>, Zisis C. Ioannidis<sup>a</sup>, Gaetano Aiello<sup>b</sup>, Patrick Bénin<sup>c</sup>, Ioannis Chelis<sup>d</sup>, Andreas Dinklage<sup>e</sup>, Gerd Gantenbein<sup>a</sup>, Stefan Illy<sup>a</sup>, John Jelonnek<sup>a</sup>, Jianbo Jin<sup>a</sup>, Heinrich P. Laqua<sup>e</sup>, Alberto Leggieri<sup>c</sup>, François Legrand<sup>c</sup>, Alexander Marek<sup>a</sup>, Stefan Marsen<sup>e</sup>, Ioannis Gr. Pagonakis<sup>a</sup>, Tobias Ruess<sup>a</sup>, Tomasz Rzesnicki<sup>a</sup>, Theo Scherer<sup>b</sup>, Dirk Strauss<sup>b</sup>, Manfred Thumm<sup>a</sup>, Ioannis Tigelis<sup>d</sup>, Dietmar Wagner<sup>f</sup>, Jörg Weggen<sup>a</sup>, Robert C. Wolf<sup>e</sup>, and the Wendelstein 7-X Team<sup>g</sup>

<sup>a,b</sup>Karlsruhe Institute of Technology (KIT),

<sup>a</sup>Institute for Pulsed Power and Microwave Technology, <sup>b</sup>Institute for Applied Materials, 76131 Karlsruhe, Germany

<sup>c</sup>Thales, Microwave & Imaging Sub-Systems, 78141 Vélizy-Villacoublay, France

<sup>d</sup>National and Kapodistrian University of Athens (NKUA), Department of Physics, 15784 Athens, Greece

<sup>e,f</sup>Max Planck Institute for Plasma Physics (IPP), <sup>e</sup>17491 Greifswald, Germany, <sup>f</sup>85748 Garching, Germany

<sup>g</sup><https://iopscience.iop.org/article/10.1088/1741-4326/ab03a7>

For the required upgrades of the Electron Cyclotron Resonance Heating system at the stellarator Wendelstein 7-X, the development of a 1.5 MW 140 GHz Continuous Wave (CW) prototype gyrotron has started. KIT has been responsible to deliver the scientific design of the tube (i.e. the electron optics design and the RF design), with contributions from NKUA and IPP. The prototype gyrotron has been ordered at the industrial partner, Thales, France, and is expected to be delivered in 2021. In parallel, a short-pulse pre-prototype gyrotron has been developed at KIT, to provide the means for a first experimental validation of the scientific design in ms pulses, prior to the construction of the CW prototype. This paper reports on the status of the 1.5 MW CW gyrotron development, focusing on the scientific design and its numerical and experimental validation.

Keywords: Gyrotron, Electron Cyclotron Resonance Heating, Wendelstein 7-X Stellarator

## 1. Introduction

The first experimental period of the stellarator Wendelstein 7-X (W7-X) showed outstanding results [1-4]. Building on a highly reliable and powerful Electron Cyclotron Resonance Heating (ECRH) system, delivering 2<sup>nd</sup> harmonic X- and O-mode heating, regimes of unexpectedly good plasma performance were achieved. This was manifested by the highest fusion triple product achieved for stellarators and pulse lengths up to 100 s. EC Current Drive was demonstrated as an efficient tool to compensate the bootstrap current in the plasma [5]. At the same time, it became clear that, for operating regimes at high plasma beta and low collisionality (as expected in reactor-scale devices and required to assess, for example, fast-ion confinement in optimized stellarators), the presently installed effective heating (~ 7.5 MW in the plasma) needs to be increased by upgrading the ECRH system to higher power. For this upgrade, a prototype Continuous-Wave (CW) 1.5 MW, 140 GHz gyrotron is under development, aiming at 30 min pulses. The prototype is planned to be followed by two series tubes. The associated power enhancement of the quasi-optical transmission line as well as the preparation of two additional gyrotron positions at W7-X are also ongoing.

Although millimeter-wave gyrotrons developed for fusion facilities like W7-X, ITER, EAST, KSTAR, JT 60SA etc. have reached the 1 MW power level in long-pulse operation, i.e. 5 s to CW ([6] and references

therein), long-pulse tubes delivering 1.5 MW CW are yet to be realized. However, as the power requirements of present and future fusion facilities (e.g. DEMO) are increasing, the research on long-pulse gyrotrons surpassing the 1 MW limit is intense worldwide. So far, notable achievements include: 110 GHz, 1.5 MW, 4 s in Japan [7], 170 GHz, 1.2 MW, 100 s in Russia [8], and 170 GHz, 1.5 MW, 2.5 s also in Russia [9]. In this context, the development of a 140 GHz, 1.5 MW 30 min gyrotron for the upgraded ECRH system at W7-X is very timely as well as challenging.

The design of the 1.5 MW gyrotron has been conceived as an upgrade of the successful design of the existing 1 MW, 140 GHz gyrotrons at W7-X [10]. This strategy ensures risk mitigation and cost control by using, or by modestly modifying, the layout of components that are already well proven in the existing W7-X tubes [11-12]. To reach the 1.5 MW goal however, significant improvements have to be realized. They include a larger cavity with an advanced cooling system, to allow for highly efficient power generation, and an improved beam tunnel to prevent excitation of parasitic modes before the cavity at the higher beam current required for 1.5 MW operation. Moreover, an adjustable 3<sup>rd</sup> mirror of the quasi-optical output coupler is foreseen, to ensure a perfect alignment of the RF beam on the gyrotron window. In addition, the high-voltage connection scheme of the mirror box has been upgraded towards even better voltage stand-off by adopting a new version of the high-voltage feedthroughs developed

during the refurbishment of the 170 GHz 1 MW CW European prototype gyrotron for ITER [13]. It should be noted that, apart from the 1.5 MW target, the listed improvements are also aiming at higher reliability, availability, maintainability and inspectability, pursuing applications in potential future fusion reactors.

The scientific design of the 1.5 MW CW prototype has been completed under the responsibility of KIT, with contributions from NKUA and IPP. (In this paper, the term “scientific design” is used for the electron optics and RF design.) To support the development of the CW prototype and to mitigate the risks, a short-pulse pre-prototype gyrotron has also been developed at KIT. This gyrotron shares the same scientific design with the CW prototype and can thus provide experimental validation of this design in ms pulses, prior to the design finalization and the construction of the CW tube. First experiments with the short-pulse tube have started at KIT in September 2020. The CW prototype has been ordered at the industrial partner, Thales, Vélizy-Villacoublay, France, with a foreseen tube delivery by August 2021.

In the following, an overview of the design of the 1.5 MW, 140 GHz CW gyrotron is given, focusing on the scientific design and its numerical and experimental validation.

## 2. Gyrotron design

### 2.1 Main considerations

The basic requirement for 1.5 MW CW at 140 GHz cannot be fulfilled with the existing 1 MW gyrotrons at W7-X, considering their limitations by design. Therefore, the development of a new prototype gyrotron is necessary. The gyrotron should be able to operate in the existing magnetic field profile of the magnets at W7-X and with the existing gyrotron power supplies. The power supplies at W7-X allow for cathode voltage  $V_{\text{cath}} < 65$  kV, beam current  $I_{\text{beam}} < 60$  A, collector depression voltage  $V_{\text{body}} < 35$  kV, and DC power  $P_{\text{DC}} < 3.3$  MW. This leads to the requirement of an overall gyrotron efficiency  $\eta_{\text{tot}} > 46\%$  (in order to achieve 1.5 MW RF power) and suggests an operating point with accelerating voltage  $V_{\text{cath}} + V_{\text{body}} \sim 80$  kV and beam current  $I_{\text{beam}} \sim 55$  A.

To keep the cost and risk of development low, it was decided to keep the overall layout of the 1.5 MW prototype gyrotron as close as possible to that of the existing 1 MW tubes at W7-X. However, in comparison to those tubes, the 1.5 MW, 140 GHz gyrotron poses a number of challenges that have to be addressed at the design stage:

(i) To increase the overall efficiency from  $> 40\%$  (existing W7-X gyrotrons) to  $> 46\%$ , the cavity design should achieve a transverse interaction efficiency close to the theoretical maximum ( $\sim 75\%$ ). Also, the undesired thermal deformation of the cavity wall should be kept as small as possible by improved cavity cooling.

(ii) To reduce the possibility of parasitic excitations in the beam tunnel at the increased current required (55-60 A, as compared to 40-45 A in the existing W7-X gyrotrons), an improved design of the stacked beam tunnel is necessary.

(iii) A 50% increase in power implies a 50% increase in internal stray radiation. To avoid this, the quasi-optical system should be further optimized to keep the stray radiation at the levels measured in the 1 MW gyrotron, despite the power increase to 1.5 MW.

Taking all the above into account, the scientific design of the 1.5 MW prototype gyrotron has been completed. Details on the design of the critical subcomponents are given in the following sections.

### 2.2 Cavity and non-linear uptaper

In order for the Ohmic loading of the cavity to be at acceptable levels ( $\sim 2$  kW/cm<sup>2</sup>) at 1.5 MW RF power, a higher-order operating mode, compared to the mode TE<sub>28,8</sub> of the existing 1 MW gyrotron, is necessary. Therefore, the selected operating mode for the 1.5 MW prototype is TE<sub>28,10</sub>. The azimuthal index  $m$  of the mode has been kept the same ( $m = 28$ ), in order for the electron beam radius to be the same as in the 1 MW tube. The cavity radius has been increased from 20.48 mm to 22.83 mm to accommodate the higher power and to make the TE<sub>28,10</sub> mode resonant at 140.35 GHz in the cold cavity. This anticipates a frequency down-shift of 300-500 MHz due to thermal expansion of the cavity.

The cavity midsection length has been increased to increase the quality factor and hence the interaction efficiency. At the nominal operating point of: magnetic field  $B_0 = 5.560$  T, beam energy  $E_b = 80$  keV, beam current  $I_b = 55$  A, electron velocity ratio  $\alpha = 1.2$ , beam radius  $R_{\text{beam}} = 10.1$  mm, and assuming an ideal electron beam without spreads, the power extracted from the electron beam is 1.9 MW at 43.2% interaction efficiency, as calculated by EURIDICE [14]. This corresponds to 73.2% transverse interaction efficiency, which is close to the theoretical maximum.

To keep the thermal deformation of the cavity wall in CW operation as small as possible and thus retain the high interaction efficiency, an improved cavity cooling circuit (as compared to the existing 1 MW W7-X tubes) has been designed by the industrial partner. In particular, the improvement aims at keeping the undesired bell-shaped deformation of the cavity as small as possible. As discussed in [15], such a deformation may reduce significantly the quality factor of the cavity and subsequently the interaction efficiency. The improvement of the cooling circuit incorporates advances already successfully implemented in the 1 MW 2 s dual frequency gyrotron for the TCX tokamak in Lausanne, Switzerland [16]. In addition to the improvements coming from the dual frequency gyrotron, the cavity cooling system is further upgraded with a specially designed water shaft, developed by the

Polytechnic University of Turin, Italy, that allows for the complete homogenization of the water velocity at the inlet of the Raschig-Rings cooling structure.

The non-linear uptaper linking the cavity to the launcher of the quasi-optical output system has been designed to minimize mode conversion of the  $TE_{28,10}$  to other modes. The calculation of the mode conversion in the non-linear uptaper is shown in Fig. 1. Clearly, at the end of the uptaper the amplitude of the spurious modes is minimal, securing a 99.95% transmission of the  $TE_{28,10}$  mode into the launcher.

The RF design of the cavity has been further validated by multi-mode simulations of the beam-wave interaction with EURIDICE, using the electron beam parameters from the electron gun design, as calculated by *Ariadne* [17] (see next section). The results are shown in Fig. 2 and the calculated nominal performance in long-pulse operation is summarized in Table 1. The calculated performance provides considerable margin with respect to the sub-optimal operating conditions occurring in reality.

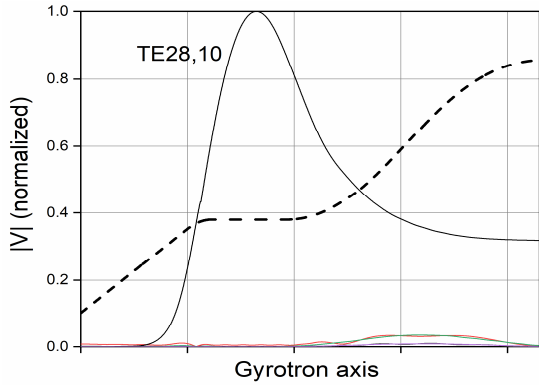


Fig. 1. Contour of cavity and non-linear uptaper of the 1.5 MW prototype along the gyrotron axis (thick dashed curve) and calculated mode conversion along the axis, shown by the normalized amplitude of the main  $TE_{28,10}$  mode (black curve) and of the spurious modes (colored curves).

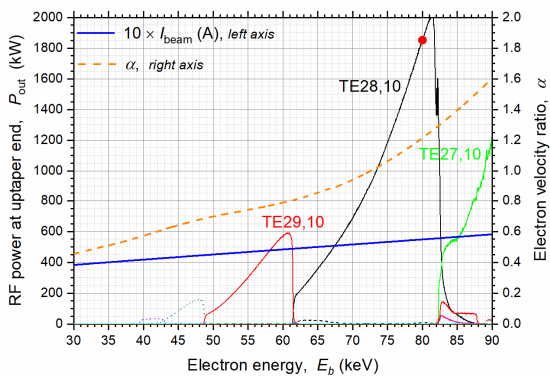


Fig. 2. Multi-mode (45 modes) simulation of the gyrotron beam-wave interaction, showing the power of different modes versus the kinetic energy of the electron beam. The nominal operating point is marked by the red point. The electron velocity ratio and the beam current are also shown.

Table 1. Calculated nominal performance of the gyrotron.

Electron kinetic energy	80 keV
Beam current	55 A
Magnetic field	5.56 T
Electron velocity ratio	1.2
Electron beam radius	10.1 mm
Accelerating voltage <sup>1</sup>	82 kV
Transverse velocity spread	2% rms
Kinetic energy spread	0.03% rms
Guiding center spread	3.6% uniform
RF power at end of uptaper	1.83 MW
Frequency	140.36 GHz
Ohmic losses <sup>2</sup>	61 kW
Maximum Ohmic wall loading <sup>2</sup>	2.2 kW/cm <sup>2</sup>
Efficiency w/o depr. collector <sup>2,3</sup>	~38.5%

<sup>1</sup>To account for a calculated partial space-charge neutralization of ~70% during long-pulse operation.  
<sup>2</sup>Assuming a correction factor of 1.8 w.r.t. ideal copper at room temperature.  
<sup>3</sup>Assuming ~5% additional losses between uptaper and window

## 2.3 Electron gun

The electron gun for the 1.5 MW gyrotron has been based on the existing electron gun of the 1 MW gyrotron at W7-X. However, careful redesign took place to secure the generation of a high-quality electron beam at increased current (55-60 A). In particular, the emitter ring has been kept identical to that of the existing W7-X gyrotrons but the contours of the cathode nose and extender have been optimized to minimize the influence that a possible emitter ring misalignment can have on the electron beam quality [18]. In addition, the axial position of the emitter ring has been shifted by ~2 cm, to eliminate the risk of formation of a beam halo by electron emission from the rear part of the cathode [19]. (It should be noted that this latter risk does not exist in the 1 MW W7-X gyrotron, because such a formation is not supported by the lower beam current and the smaller cavity radius.) The anode has also been redesigned to reach the required beam parameters at the nominal operating point. An excellent beam quality with very low transverse velocity spread ( $\delta\beta_{\perp} < 2\%$  rms) has been verified by simulation. The electron gun has been designed using *Ariadne* and has been numerically validated using *Ariadne* and ESRAY [20]. Simulation results are shown in Fig. 3.

## 2.4 Beam tunnel

The beam tunnel of the existing 1 MW gyrotrons at W7-X follows the stacked concept of alternating dielectric absorbing rings and indented copper rings [21]. This beam tunnel has offered satisfactory suppression of parasitic oscillations at the operating beam current (40-45 A) of the 1 MW gyrotron. However, the 1.5 MW gyrotron requires higher beam current, of the order of 55-60 A. In order to mitigate the risk of parasitic mode excitation by beam currents of that order, a new baseline beam tunnel has been designed, using the code NESTOR

[22]. Although the BeO/SiC ceramic material for the absorbing rings has been kept the same as in the beam tunnel of the 1 MW gyrotron, the geometry of the dielectric and copper rings has been optimized according to the recent findings of [23] and a considerable increase of the diffraction losses of the possible parasitic modes has been achieved. According to cold-cavity calculations, the performance of the new baseline beam tunnel is improved by approximately 25% (in terms of number and quality factor of potential parasitic modes in the frequency range of 115-135 GHz), compared to the beam tunnel of the 1 MW gyrotron.

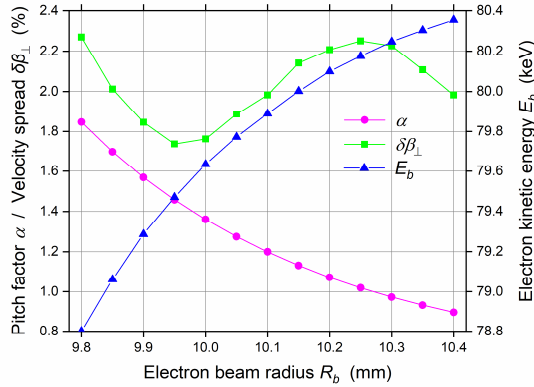


Fig. 3. Electron gun simulation at 55 A beam current and 82 kV accelerating voltage with *Ariadne*: calculated electron velocity ratio  $\alpha$ , rms transverse velocity spread  $\delta\beta_{\perp}$ , and electron kinetic energy  $E_b$  as functions of the electron beam radius. (The nominal beam radius of the 1.5 MW gyrotron is 10.1 mm.)

An alternative, further improved beam tunnel has also been designed [24]. It uses BeO/SiC ceramic material of different concentration, following the theoretical guidelines of [25], which have been recently validated experimentally [26]. The performance of this alternative design, in terms of number and quality factor of possible parasitics in the frequency range of 115-135 GHz, is improved by approximately 50%, compared to the beam tunnel of the 1 MW gyrotron. This is evident in Fig. 4, where the quality factors and the frequencies of the resonant modes in the beam tunnel are shown. The selected frequency band (115-135 GHz) is where parasitic excitation due to electron cyclotron resonance in the beam tunnel is possible. The number of resonant modes with quality factor  $Q > 60$  in the alternative design for the 1.5 MW gyrotron is  $N = 419$  and the highest quality factor encountered is  $Q_{\max} = 170$ . The corresponding numbers for the existing beam tunnel of the 1 MW gyrotron are  $N = 1135$  and  $Q_{\max} = 267$ , respectively.

The decision on which beam tunnel design (baseline or alternative) will be incorporated in the 1.5 MW CW prototype gyrotron will be taken after comparing the experimental performance of both designs in the short-pulse pre-prototype gyrotron (see section 3).

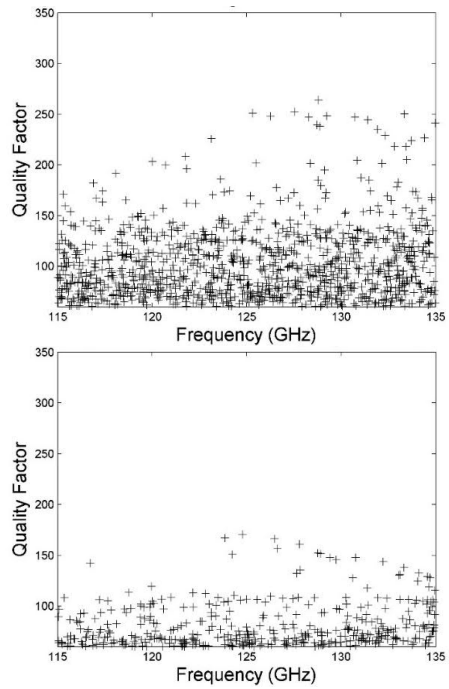


Fig. 4. Cold-cavity calculation of frequencies and quality factors  $Q$  of resonant parasitic modes with  $Q > 60$  in the existing beam tunnel of the 1 MW gyrotron at W7-X (top) and in the alternative beam tunnel design for the 1.5 MW gyrotron (bottom). The improvement offered by the alternative design is apparent.

## 2.5 Quasi-optical system

A mirror-line launcher [27] and three mirrors with quasi-quadratic surface contour function (for the conversion of the operating  $TE_{28,10}$  mode to a Gaussian RF beam at the gyrotron window) have been designed using TWLDO, an in-house code developed at KIT, and the commercial code SURF3D. The schematic of the quasi-optical system is shown in Fig. 5. The simulated field distribution on the launcher wall and at the window plane is shown in Fig. 6. An excellent performance has been achieved by the design, with a calculated Gaussian mode content of 99% at the window and with calculated stray radiation levels as low as 1.65%. The performance of the quasi-optical system is summarized in Table 2. The 3<sup>rd</sup> mirror of this quasi-optical output coupler will be steerable to ensure perfect alignment of the RF beam on the window. This concept has already been successfully demonstrated by the industrial partner [16].

## 2.6 Window and collector

Given that the frequency of the 1.5 MW, 140 GHz gyrotron will be same to that of the existing 1 MW gyrotrons at W7-X, the design of the Chemical Vapor Deposition (CVD) diamond window for the upgraded gyrotron is practically the same to that of the 1 MW tubes. It features a CVD diamond disk with a 1.8 mm thickness and 106 mm diameter, brazed to two copper cuffs of 1 mm thickness. The brazed disk is enclosed in a

stainless steel housing. The window has an aperture of 88 mm and the edge of the disk is directly in contact with the coolant.

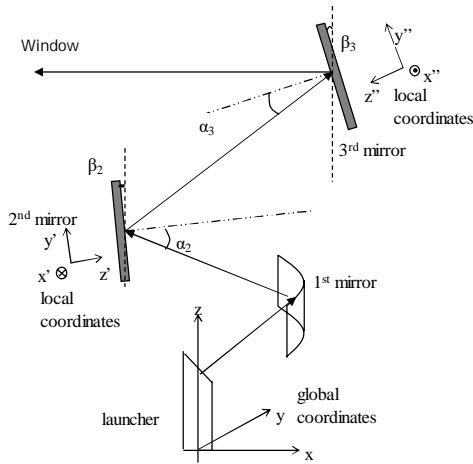


Fig. 5. Schematic of the quasi-optical system of the 1.5 MW gyrotron.

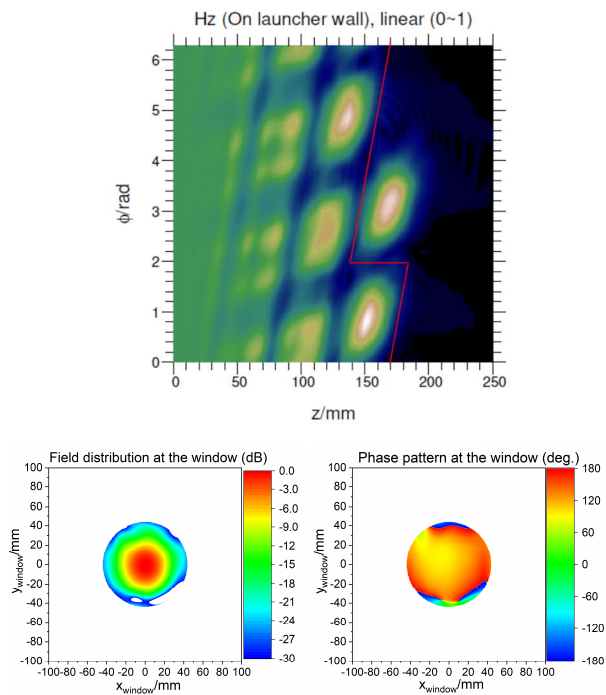


Fig. 6. Top: simulated RF field amplitude on the launcher wall. The launcher cut is shown by the red line. Bottom: Simulated amplitude (left) and phase (right) of the RF field distribution at the window.

In view of the higher power, however, as well as of the plan to use silicone oil cooling (to avoid a possible corrosion in the long term that water cooling could cause), a series of CFD conjugated heat transfer and structural analyses have been performed, using the commercial code ANSYS V19.2. The target has been to

assess the behavior of the window assembly at 1.5 MW operation with oil cooling. The heat transfer analyses validated the performance of the cooling system: even assuming the “worst-case” of 1.5 kW absorption from the diamond disk (corresponding to a loss tangent of  $5.68 \times 10^{-5}$ ), a maximum temperature below  $215^\circ\text{C}$  at the disk center has been calculated, as shown in Fig. 7. This is well below the conservative limit of  $250^\circ\text{C}$  for diamond. In addition, despite the asymmetric temperature profile observed on the window disk (i.e.  $\sim 20^\circ\text{C}$  difference at the two edges of the disk due to the high turbulent kinetic energy of the fluid right after the inlet pipe), the structural analyses indicated thermal stresses well below the critical limits both in the disk and in the cuffs. A comprehensive account of the extensive studies reported above can be found in [28].

Table 2. Calculated performance of the quasi-optical system.

Gaussian mode content at window plane	99.0%
Stray radiation	1.65%
Max. Ohmic loading of launcher wall*	0.53 kW/cm <sup>2</sup>
Beam waist, $w_x$	21.67 mm @ 190.4 mm after window
Beam waist, $w_y$	21.69 mm @ 201.6 mm after window
Beam radius at window	$R_x = 22.48, R_y = 22.59$
*Assuming a correction factor of 1.8 w.r.t. ideal copper at room temperature.	

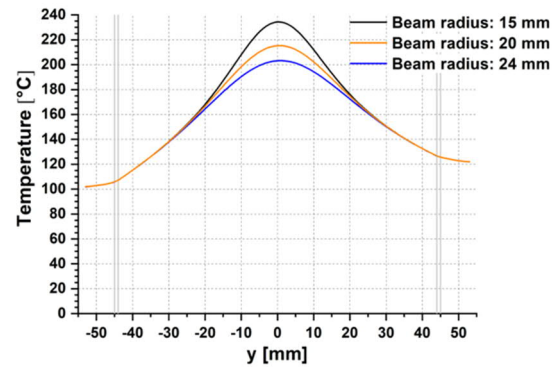


Fig. 7. Calculated temperature profile along the oil-cooled CVD diamond disk for three values of the RF beam radius, assuming a “worst-case” of 0.1% absorption at 1.5 MW RF power. For the nominal value of the RF beam radius ( $\sim 22.5$  mm) a maximum temperature below  $215^\circ\text{C}$  is expected. The y-axis is the inlet - outlet axis of the coolant, hence the  $\sim 20^\circ\text{C}$  difference at the two edges of the disk. The vertical lines represent the copper cuffs brazed to the disk.

The collector design for the 1.5 MW prototype will also be practically the same to that of the 1 MW W7-X gyrotrons. It is foreseen that this collector can handle the expected  $\sim 50\%$  increase in the power of the spent electron beam at 1.5 MW operation. Nevertheless, to

further improve the homogeneity of the loading on the collector wall, sophisticated schemes for the vertical magnetic sweeping of the electron beam are planned, based on the findings of [29]. Transversal beam sweeping is also foreseen, as is the case for the existing 1 MW W7-X tubes.

### 3. Experimental validation of the scientific design

To support the development of the 1.5 MW 140 GHz CW prototype gyrotron, a modular short-pulse gyrotron has in parallel been designed and fabricated at KIT. The electron gun for this gyrotron has been procured at Thales. The scientific design of the short-pulse tube is identical to that of the 1.5 MW CW prototype. In this way, the operation of the short-pulse gyrotron can provide the first experimental validation of the scientific design of the individual gyrotron components as well as of the overall gyrotron performance in ms pulses. The components of the short-pulse gyrotron are assembled together with flanges and, with the exception of the collector and the cathode, are not actively cooled. This makes the construction much simpler than the CW tube and offers the opportunity of experimentally testing different versions of gyrotron components at a short time scale. Other differences with respect to the CW prototype include a short-pulse collector of smaller dimensions, main and relief windows made of quartz (Infrasil 302), and a non-steerable 3<sup>rd</sup> mirror.

Prior to the installation in the short-pulse gyrotron, the complete quasi-optical system (i.e. launcher and three mirrors) has been tested in low power at the KIT test bench. For this purpose, a dedicated mode generator for the generation of the operating  $TE_{28,10}$  mode has been developed [30], [10]. The mode generator is driven by a Vector Network Analyser (VNA) and a waveguide antenna is used, in order to record the amplitude and the phase of the radiated electric field at a distance that corresponds to the plane of the gyrotron output window. The installation of the quasi-optical system at the KIT test bench is shown in Fig. 8. The measurements were performed with a network analyzer PNA 5222B at 140.02 GHz. The field amplitude and phase at the window plane, measured with a step size of 0.5 mm, are shown in Fig. 9.

The low-power measurements validated the RF design of the quasi-optical system. After post-processing of the measurements, the Gaussian mode content of the RF beam, taking into account both the amplitude and the phase and considering a window diameter of 88 mm, has been estimated to be higher than 97%. The small difference to the design value (Table 2) is most probably due to the non-perfect low-power mode generation and, in addition, to the manufacturing tolerances.



Fig. 8. Assembly of the quasi-optical system for the low-power measurements.

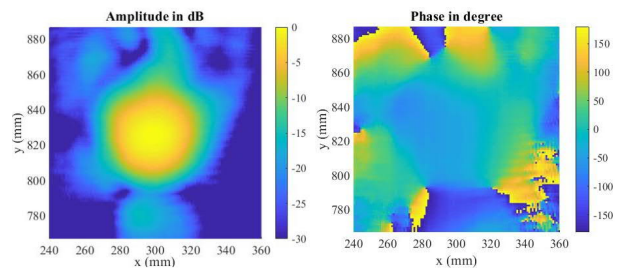


Fig. 9. Low-power measurements with the complete quasi-optical system: amplitude (left) and phase (right) of the RF field at the window plane.



Fig. 10. The first configuration of the 1.5 MW 140 GHz short-pulse gyrotron before (left) and after (right) installation at the KIT gyrotron test stand.

Following the low-power tests of the quasi-optical system, the first configuration of the short-pulse gyrotron was assembled and installed in the super-conducting magnet at the KIT gyrotron test stand. (Fig. 10). This configuration incorporates the new baseline beam tunnel. The first experimental campaign with RF generation took place in September 2020. The design target of

1.5 MW RF power was clearly achieved with very good efficiency, both with and without collector depression, in pulses of 0.5-1.0 ms. These results validated the scientific design of the gun, the beam tunnel, and the cavity. A detailed account of the first experimental campaign is given in [31].

#### 4. Summary and outlook

The development of a 1.5 MW 140 GHz CW prototype gyrotron operating in the  $TE_{28,10}$  mode is ongoing, in the framework of a power upgrade of the ECRH system at the stellarator W7-X. The scientific design (i.e. the beam optics and RF design) of all gyrotron components has been completed and has been validated numerically by in-house and commercial codes. The RF design of the quasi-optical system has also been validated experimentally with low-power measurements, using a mode generator for the  $TE_{28,10}$  mode. The experimental validation of the scientific design of all critical gyrotron components, by means of a short-pulse pre-prototype gyrotron at KIT, has already started. So far, the results are very good and confirm the design of the electron gun, the baseline beam tunnel, and the cavity. The experimental campaign will continue with measurements of the RF beam and the stray radiation, in order to validate the quasi-optical system design also in the high-power regime. The next configuration of the short-pulse gyrotron is planned to include the alternative beam tunnel. Following these tests, the beam tunnel with the best performance will be incorporated in the CW prototype tube, which is under manufacturing at Thales, France. The CW prototype gyrotron is expected to be delivered in August 2021. Prospects for future reactor-scale applications will also be assessed.

#### Acknowledgments

This work has been carried out within the framework of the EUROfusion Consortium and has received funding from the Euratom research and training programme 2014-2018 and 2019-2020 under grant agreement No 633053. The views and opinions expressed herein do not necessarily reflect those of the European Commission. The fabrication of the short-pulse pre-prototype gyrotron has been supported by Innovationspool (“W7-X HiPower”), Bundesministerium für Bildung und Forschung, Germany. Part of the simulations was performed on the EUROfusion High Performance Computer (Marconi-Fusion).

#### References

[1] T. Klinger et al., Overview of first Wendelstein 7-X high-performance operation, *Nuclear Fusion* 59 (2019) 112004.  
 [2] R. C. Wolf et al., Electron-cyclotron-resonance heating in Wendelstein 7-X: A versatile heating and current-drive method and a tool for in-depth physics studies, *Plasma Physics and Controlled Fusion* 61 (2019) 014037.

[3] R. C. Wolf et al., Performance of Wendelstein 7-X stellarator plasmas during the first divertor operation phase, *Physics of Plasmas* 26 (2019) 082504.  
 [4] A. Dinklage et al., Magnetic configuration effects on the Wendelstein 7-X stellarator, *Nature Physics* 14 (2018) 855-860. <https://doi.org/10.1038/s41567-018-0141-9>  
 [5] Yu. Turkin et al., *in preparation*.  
 [6] M. K. A. Thumm et al., High-power gyrotrons for electron cyclotron heating and current drive, *Nuclear Fusion* 59 (2019) 073001.  
 [7] T. Kobayashi et al., Progress of high-power and long-pulse ECRF system development in JT-60, *Nuclear Fusion* 51 (2011) 103037.  
 [8] A. G. Litvak et al., New results of megawatt power gyrotrons development, *proc. 38<sup>th</sup> International Conference on Infrared, Millimeter, and Terahertz Waves*, 1-6 September 2013, Mainz, Germany. DOI: 10.1109/IRMMW-THz.2013.6665555  
 [9] V. E. Myasnikov et al., New results of extra-powerful 1.5MW/170GHz gyrotron development, *proc. 39<sup>th</sup> International Conference on Infrared, Millimeter, and Terahertz Waves*, 14-19 September 2014, Tucson, AZ, USA. DOI: 10.1109/IRMMW-THz.2014.6956474  
 [10] K. A. Avramidis et al., Studies towards an upgraded 1.5 MW gyrotron for W7-X, *EPJ Web of Conferences* 203 (2019) 04003.  
 [11] V. Erckmann et al., Electron cyclotron heating for W7-X: physics and technology, *Fusion Science & Technology* 52 (2007) 291.  
 [12] M. Thumm et al., Progress in the 10-MW 140-GHz ECH system for the stellarator W7-X, *IEEE Transactions on Plasma Science* 36 (2008) 341-355.  
 [13] Z. C. Ioannidis et al., Recent experiments with the European 1MW, 170GHz industrial CW and short-pulse gyrotrons for ITER, *Fusion Engineering and Design* 146 (2019) 349-352.  
 [14] K. A. Avramides et al., EURIDICE: A code-package for gyrotron interaction simulations and cavity design, *EPJ Web of Conferences* 32 (2012) 04016.  
 [15] K. A. Avramidis et al., Numerical studies on the influence of cavity thermal expansion on the performance of a high-power gyrotron, *IEEE Transactions on Electron Devices* 65 (2018) 2308 - 2315.  
 [16] R. Marchesin et al., Manufacturing and test of the 1 MW long-pulse 84/126 GHz dual-frequency gyrotron for TCV, *20<sup>th</sup> International Vacuum Electronics Conference*, 28 April - 1 May 2019, Busan, South Korea. <https://doi.org/10.1109/IVEC.2019.8745147>  
 [17] I. Gr. Pagonakis et al., The self-consistent 3D trajectory electrostatic code Ariadne for gyrotron beam tunnel simulation, *proc. 29<sup>th</sup> Joint International Conference on Infrared and Millimeter Waves and THz Electronics*, 27 September - 1 October 2004, Karlsruhe, Germany, 657-658.  
 [18] I. Gr. Pagonakis et al., Influence of emitter ring manufacturing tolerances on electron beam quality of high power gyrotrons, *Physics of Plasmas* 23 (2016) 083103.  
 [19] I. Gr. Pagonakis et al., Electron trapping mechanisms in

- magnetron injection guns, *Physics of Plasmas* 23 (2016) 023105.
- [20] S. Illy et al., Gyrotron electron gun and collector simulation with the ESRAY beam optics code, 2015 IEEE International Vacuum Electronics Conference, 27-29 April 2015, Beijing, China. DOI: 10.1109/IVEC.2015.7223779
- [21] G. Gantenbein et al., Experimental investigations and analysis of parasitic RF oscillations in high-power gyrotrons, *IEEE Transactions on Plasma Science* 38 (2010) 1168–1177.
- [22] I. G. Chelis et al., Resonant modes of disk-loaded cylindrical structures with open boundaries, *IEEE Transactions on Microwave Theory and Techniques* 63 (2015) 1781–1790.
- [23] I. G. Chelis et al., Increasing the diffraction losses in gyrotron beam tunnels for improved suppression of parasitic oscillations, *proc. 44<sup>th</sup> International Conference on Infrared, Millimeter and Terahertz Waves*, 1 - 6 September 2019, Paris, France. DOI: 10.1109/IRMMW-THz.2019.8874402
- [24] I. G. Chelis et al., Final Report on Deliverable S1-WP19-20.IH-T004-D003: Interim report on design and validation of beam tunnel for the 1.5 MW 140 GHz gyrotron (NCSR), EUROfusion IDM, EFDA\_D\_2MZ5UE, *available upon request*.
- [25] I. G. Chelis et al., Improved suppression of parasitic oscillations in gyrotron beam tunnels by proper selection of the lossy ceramic material, 65 (2018) 2301 - 2307.
- [26] Z. C. Ioannidis et al., Experimental classification and enhanced suppression of parasitic oscillations in gyrotron beam tunnels, *IEEE Transactions on Electron Devices* (2020), *accepted for publication*.
- [27] J. Jin et al., Novel numerical method for the analysis and synthesis of the fields in highly oversized waveguide mode converters, *IEEE Transactions on Microwave Theory and Techniques* 57 (2009) 1661.
- [28] G. Aiello et al., Design validation of the gyrotron diamond output window for the upgrade of the ECRH system at W7-X, 31<sup>st</sup> Symposium on Fusion Technology, 20-25 September 2020, *to appear in Fusion Engineering and Design*.
- [29] S. Illy et al., Optimized vertical collector sweeping for high power CW gyrotrons using advanced current waveforms, 43<sup>rd</sup> International Conference on Infrared, Millimeter and Terahertz Waves, 9 -14 September 2018, Nagoya, Japan. <https://doi.org/10.1109/IRMMW-THz.2018.8509998>
- [30] T. Ruess et al., Computer-controlled test system for the excitation of very high-order modes in highly oversized waveguides, *Journal of Infrared, Millimeter, and Terahertz Waves* 40 (2019) 257–268.
- [31] Z. C. Ioannidis et al., “Generation of 1.5MW-140GHz ms pulses with the modular pre-prototype gyrotron for W7-X”, *to be submitted to IEEE Electron Device Letters*.